Subchromophore interactions in tricyanovinyl-substituted triarylamines—a combined experimental and computational study

Christoph Lambert,*[a] Wolfgang Gaschler,[a] Elmar Schmälzlin,[b] Klaus Meerholz[b] and Christoph Bräuchle[b]

[a] *Institut für Organische Chemie, Universität Regensburg, Universitätsstraße 31, D-93040 Regensburg, Germany. Fax: +49 (0)941/943 4984, E-mail: christoph.lambert@chemie.uni-regensburg.de*

[b] *Lehrstuhl für Physikalische Chemie, Ludwig-Maximilians-Universität München, Sophienstraße 11, 80333 München, Germany*

Received (in Cambridge) 15th October 1998, Accepted 14th January 1999

The electronic coupling between the phenyl substituents of mono-, bis-, and tris(tricyanovinyl)-substituted triphenylamines (**1**, **2**, **2-OMe** and **3**) have been investigated by various methods: the splitting of excited states was taken as a measure of the interaction. These splittings can be seen in the optical absorption spectra; exciton coupling theory was also used to estimate electronic coupling of the excited states; redox potentials gave coupling energies of charged ground state species as well as Hush analysis of intervalence charge-transfer bands (IV-CT), which were observed by UV-Vis-NIR spectroelectrochemistry, and finally, the quadratic hyperpolarisability measured by hyper-Rayleigh scattering was used to estimate excited state couplings. The results of these methods were compared to semiempirical AM1 calculations and suggest the subchromophore interactions to be weak compared to the band width of the UV-spectra. Nevertheless, the quadratic hyperpolarisability is enhanced in the two-dimensional tris(tricyanovinylphenyl)amine compared to its one-dimensional analogue.

Introduction

Electronic coupling of molecular subunits is of great importance for electron and energy transfer processes in biological systems, *e.g.* the photosynthetic reaction centre,[1] but also for the design of artificial optoelectronic devices. For this reason, the redox and intermolecular electron transfer properties of triarylamines have been widely explored because those derivatives being reversibly oxidisable[2] can be used as hole transport components in *e.g.* organic light-emitting devices (OLED) or xerographic processes.[3]

Triarylamines are one of the prototypes of two-dimensional chromophores.[4] In principal, substituted triarylamines can either be viewed as delocalised two-dimensional π-electron systems (superchromophore), where delocalisation of the phenyl rings occurs *via* the central nitrogen p-orbital, or, alternatively, as composite chromophores, comprised of three weakly interacting phenyl branches. Despite the above mentioned practical importance of triarylamines, it is still unclear whether these derivatives behave as delocalised superchromophores or as composite chromophores. The early interpretation by Jaffe[5] that in Ph_3N "extensive delocalisation between phenyl radicals occurs" was based on UV spectra of Ph_3N, Ph_2NCH_3, and $PhN(CH_3)_2$ but can be questioned because these derivatives cannot be compared on the same level: a dimethylamino group has a different electron donor strength and induces different steric hindrance than a diphenylamino group. The latter point is crucial as this enforces a propeller-like geometry in the triphenylamine.[2b] On the other hand, the observation that excited singlet and triplet triphenylamine have a considerable dipole moment (*ca.* 2–3 D)[6] might lead to the assumption that an optical excitation is localised within one phenyl branch and, thus, the chromophore cannot be regarded as fully delocalised.

Two-dimensional chromophores in general have attracted much attention during recent years because of their potential use as chromophores with second-order nonlinear optical properties.[7,8] In contrast to one-dimensional systems where only one β tensor component is significant (β_{zzz} along the molecular axis), two-dimensional chromophores have (depending on the symmetry) several nonzero off-diagonal elements, *i.e.* octupolar contributions. The particular interest in two-dimensional nonlinear optical (NLO) chromophores stems from the observation that these systems may have higher optical nonlinearities at shorter absorption wavelengths than their 1D counterparts. Due to the lack of a ground state dipole moment, the preferential crystallisation in acentric space groups (a necessity for observing macroscopic second-order nonlinear optical effects) might be enhanced compared to dipolar compounds.[8]

Recently, acceptor-substituted triarylamines have been investigated as 2D-NLO-chromophores with purely octupolar contributions to the quadratic hyperpolarisability tensor.[9] These compounds were compared with one-dimensional acceptor-substituted dimethylanilines and an enhancement of optical nonlinearity was found in the triarylamine derivatives. However, the comparison is not entirely fair because of the different electronic and steric properties of triarylamines and anilines as mentioned above. Therefore, we decided to synthesise mono-, bis-, and tris(tricyanovinyl)-substituted triphenylamines (**1**, **2**, and **3**) which should allow a better comparison. The tricyanovinyl groups were chosen so as to ensure reversible reduction of the chromophore branches. For comparison, a triphenylamine with two tricyanovinyl acceptor groups and one methoxy donor group was also synthesised.

Our aim was to assess the extent of interactions between the substituted phenyl units in triarylamines. Several methods were used to investigate these interactions: orbital and excited state splittings are used as a measure for the coupling.[10] The former were calculated by the semiempirical AM1 method, the latter were taken from optical absorption spectra; exciton coupling can be used to estimate electronic coupling of excited states;[11] redox potentials measured by *e.g.* cyclic voltammetry give coupling energies of charged ground state species; Hush analysis[12] of intervalence charge-transfer bands (IV-CT), which are observable by UV-Vis-NIR spectroelectrochemical experiments also

Table 1 Absorption maxima ($\tilde{\nu}_{max}$/cm^{-1}) of **1–3** in different solvents. Values in italics are AM1-CISD(6,3) computed

	Gas	Ether	Dioxane	THF	Ethyl acetate	$CHCl_3$	Acetone	DMSO	MeCN	ε/cm^{-1} M^{-1} [a]	f [b]	$\tilde{\nu}_{1/2}$ [c]/ cm^{-1}
1		19660	19770	19510	19600	18870	19520	19220	19410	33100	0.55	3530
	25700	*20440*							*19270*		*0.27*	
2		18430*y*	18930*y*	18640*y*	18720*y*	18080*y*	18540*y*	18130*y*	18350*y*	30800*y*	0.32	2390
		20930*z*	21350*z*	21050*z*	21280*z*	20560*y*	21120*z*	20680*z*	20900*z*	15800*z*	0.33	4800
	25900y [d]								*19870y*		*0.57*	
	29360z								*20310z*		*0.07*	
2-OMe		18430*y*	18510*y*	18870*y*	18250*y*	17650*y*	18090*y*	17730*y*	17920*y*	30900*y*	0.35	2650
		20920*z*	20940*z*	20820*z*	20750*z*	20210*z*	20610*z*	20100*z*	20450*z*	17600*z*	0.37	4870
	25530y [d]	*19220y*							*18810y*		*0.83*	
	28970z	*19740z*							*19290z*		*0.05*	
3		19950	19950	19710	19630	19340	19400	18970	19160	55600	0.93	3610
	28920	*20600*							*20470*		*0.98*	
DFPA [e]									26420*y*			2290
									31020*z*			4730

[a] Molar absorptivity in MeCN. [b] Oscillator strength in MeCN. [c] Band width at half-height in MeCN. [d] Polarisation in *y* and *z* directions. [e] Di(4-formylphenyl)phenylamine.

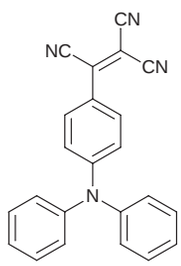

1

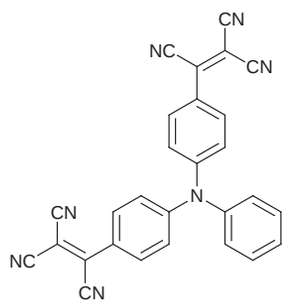

2

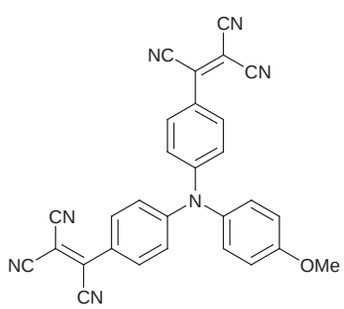

2-OMe

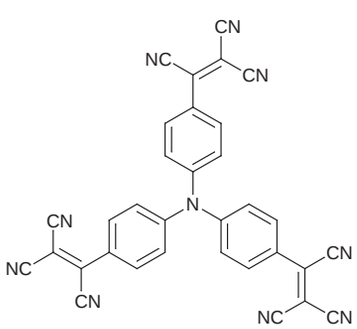

3

gives coupling energies of charged species, and finally, the quadratic hyperpolarisability measured by hyper-Rayleigh scattering[13,14] gives information about excited state coupling. The results of these methods were compared to semiempirical AM1 calculations.

Results and discussion

A. Synthesis

The synthesis of 4-(tricyanovinyl)phenyl(diphenyl)amine **1** is straightforward and can be accomplished by electrophilic aromatic substitution of triphenylamine by tetracyanoethylene in DMF. Although traces of disubstituted product can be detected by thin-layer chromatography, the di- and trisubstituted triphenylamine cannot be synthesised in this way, not even in the presence of an excess of tetracyanoethylene and prolonged reaction times. This behaviour suggests that the electron density is reduced in the monosubstituted triphenylamine with the consequence that the second substitution reaction is slowed down. Thus, a certain amount of interaction between the phenyl branches is obvious. For the synthesis of the di- and trisubstituted derivatives **2**, **2-OMe**, and **3**, the alternative route *via* the corresponding 4-formylphenylamines, Knoevenagel reaction with malonodinitrile, addition of CN^- to the dicyanovinyl group and finally oxidation with $Pb(OAc)_4$ was followed (see Scheme 1).[15] The respective formyltriphenylamines have been

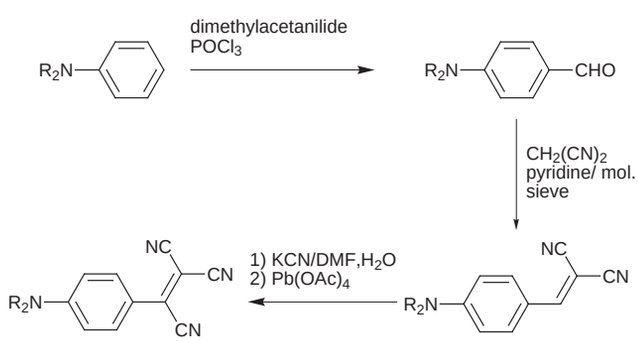

Scheme 1

synthesised by Vilsmeier formylation according to known procedures (see Experimental section). Compounds **1–3** are dark violet solids which readily dissolve in moderately polar to strong polar aprotic solvents. In protic media, decomposition occurs within minutes to hours.

B. Linear optical properties

UV-Vis spectra of compounds **1**–**3** were recorded in several aprotic solvents. All compounds show intense charge-transfer (CT) bands around 500 nm (see Fig. 1 and Table 1). The absorption maxima of **1** and **3** correlate nicely with the E_T^N Dimroth–Reichardt solvent parameter[16] for ether, dioxane, THF, ethyl acetate, acetone, MeCN and DMSO (Fig. 2). The correlation is somewhat worse for **2** and **2-OMe**. The value for $CHCl_3$ is not in line with this correlation, probably due to Cl_3C–H hydrogen bond interactions to the CN groups; these data are therefore omitted in Fig. 2. Surprisingly, the λ_{max} values of **1** and **3** do not deviate much (*e.g.* $\Delta\tilde{\nu}$ = 250 cm^{-1} in MeCN).

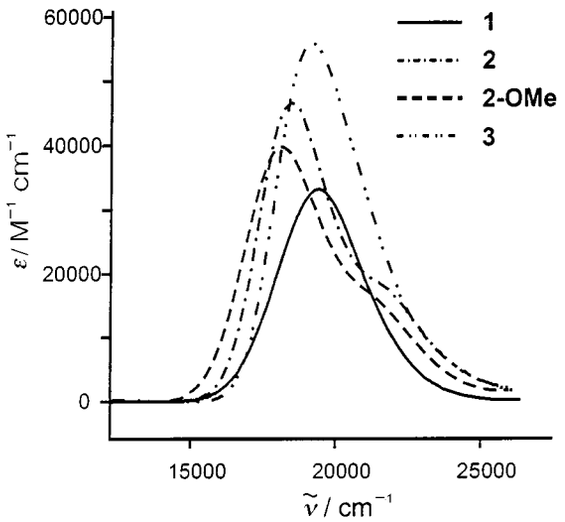

Fig. 1 UV-Vis spectra of **1**–**3** in MeCN.

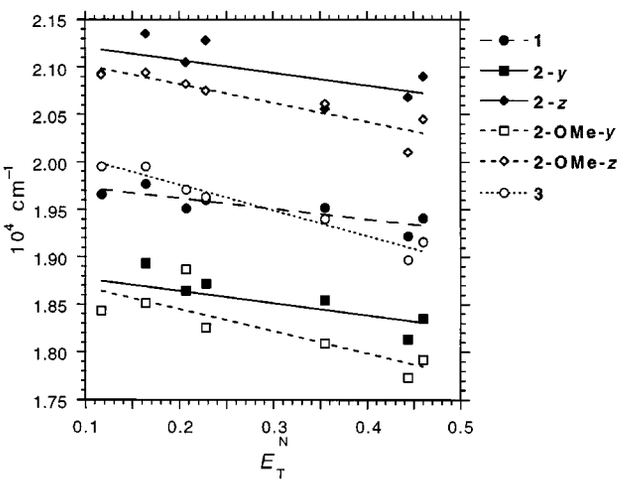

Fig. 2 Solvatochromism of compounds **1**–**3**. The solvents are from left to right: ether, dioxane, THF, ethyl acetate, acetone, DMSO, MeCN.

For simplicity, in the following we assume D_3 symmetry for **3** and C_2 symmetry for **2** and **2-OMe**. Although the geometries of **2**, **2-OMe** (actually C_1), and **3** (actually C_3) deviate from these point groups due to the tricyanovinyl groups, the (localised) transition moments should follow the assumed symmetry.

The spectra of **2** and **2-OMe** show besides the very intense CT band a shoulder at higher energy (see Fig. 1). The positions of these bands in different solvents were estimated by fitting the spectra with two Gaussian functions. As in similar cases (*e.g.* malachite green),[4,17] the intense low energy band can be assigned to the *y*-polarised (perpendicular to the molecular axis, B state) transition and the weaker, high energy band to the *z*-polarised (along the molecular axis, A state) transition. Both the *y*- and the *z*-bands show solvatochromism which is stronger for the methoxy derivative **2-OMe** than for **2** (see Fig. 2).

Although **3** should have a zero ground state dipole moment due to the approximate D_3 symmetry (AM1 calculation: 0.6 D), it shows significant solvatochromism [$\Delta\tilde{\nu}(\text{MeCN–ether})_{exp}$ = 790 cm^{-1}], even more pronounced than **1** [$\Delta\tilde{\nu}(\text{MeCN–ether})_{exp}$ = 250 cm^{-1}]. An explanation would be a solvent induced symmetry breaking, which leads to a nonzero dipole moment in the ground state.[17] Although this symmetry distortion might be very small, a possible consequence is that the branches in **3** are excited separately, *i.e.* an exciton is localised in a single branch. An alternative explanation suggests an intrinsically localised exciton without solvent induced symmetry breaking which leads to a polar excited state. Recent studies of *e.g.* tris-(bipyridine)ruthenium(II) support the latter mechanism.[18] A prerequisite for both mechanisms is a small electronic coupling between the chromophore branches compared to the band width at half-height. As we will see below, the coupling in **2**,**2-OMe** and **3** is indeed much smaller than the observed band widths (see Table 1).[19]

Interestingly, the ratio between the oscillator strengths of **1** and **3** (calculated from the absorption band integral and $f = 4.319 \times 10^{-9} \int \varepsilon(\tilde{\nu}) d\tilde{\nu}$) is close to 1:2 rather than 1:3 as expected in such a case (see Table 1). This might be due to the fact that **3** is not just three molecules of **1** arranged in a symmetrical way but is rather an extension of **1** by two additional tricyanovinyl groups where both **1** and **3** share the same number of phenyl groups. However, the alternative 1D-model compound with alkyl substituents attached to the amine nitrogen suffers from different steric and electronic interactions between the *N*-substituents (see Introduction). The *y*- and *z*-polarised bands of **2** and of **2-OMe** possess very similar oscillator strengths, the sum of both being *ca.* two-thirds that of the CT band of **3** (see Table 1).

According to an AM1 calculated orbital diagram (Scheme 2),

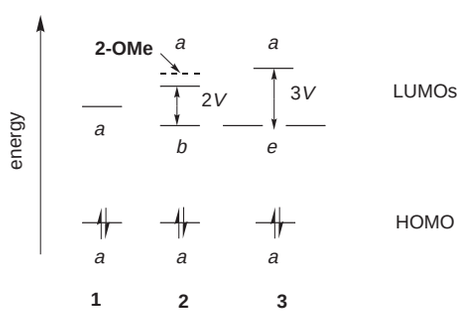

Scheme 2

the HOMO of **1** is mainly formed by the nitrogen lone-pair orbital, whereas the LUMO is localised at the tricyanovinyl π-orbitals. The interaction of two tricyanovinylphenyl (TCV-phenyl) groups in **2** and **2-OMe** results in a splitting of the LUMOs. The splitting of the LUMO and LUMO+1 is a measure for the coupling of the chromophore branches which is $2V$ (V is the coupling integral) for **2** and **2-OMe**. Accordingly, the interaction in **3** leads to a splitting of the LUMOs into a set of degenerate e-orbitals and one a-orbital. For symmetry reasons, $\Delta E(\text{LUMO}_a - \text{LUMO}_e) = 3V$. This orbital diagram corresponds qualitatively to the electronic state diagram for **2**, **2-OMe** and **3** if electron–electron interactions are omitted (Hückel theory). A small coupling leads to a small energy lowering of the e-type LUMOs (and the E excited states), and consequently to a small red shift in the absorption spectrum as observed in MeCN for **3** *vs.* **1**. As the splitting of the excited states is a measure of the electronic coupling between the subunits, it allows the direct determination of V from the UV-Vis spectra of **2** and **2-OMe** which is $1/2(E_A - E_B) = 1280$ cm^{-1} for **2** and 1270 cm^{-1} for **2-OMe**. For **3**, the transition to the *A* state is forbidden by symmetry, and, therefore, the coupling cannot be evaluated from the UV-spectrum.

Using semiempirical AM1-CISD calculations one can estimate the electronic coupling in **1**–**3** by computing the energy difference of the excited states or by calculating the splitting energy of the LUMOs,[20] the latter being systematically much smaller (*ca.* 400–500 cm^{-1}) than the state splittings in the gas phase (1200–1700 cm^{-1}). These gas phase values are in good agreement with the experimental couplings from band splittings of **2** and **2-OMe**. The results of both methods for **2**, **2-OMe** and **3** are collected in Table 2.

As the transition energies of dipolar molecules are very sensitive to the surrounding medium, we performed self-consistent reaction-field calculations (SCRF) in order to simulate the sol-

Table 2 Coupling energies (V/cm^{-1}) estimated by various methods

	AM1 LUMO/ LUMO-1 splitting (gas phase)	AM1 CISD(6,3) state splitting (gas/MeCN)	Exp. UV band splitting (MeCN)	Exciton coupling	CV redox potential splitting	Hush IV-CT band shape analysis
2-OMe	496	1722/242	1270		710	310
2	480	1730/222	1280		665	170
3	411	1202/828		610	500	160

vent influence. The calculated λ_{max} values in MeCN are in very good agreement with the experimental ones. For compound **1**, the calculated solvatochromism is much stronger than the experimental: [$\Delta\tilde{\nu}$(MeCN–ether)$_{exp} = -250$ cm^{-1}, $\Delta\tilde{\nu}$(MeCN–ether)$_{AM1} = -1170$ cm^{-1}] (see Table 1). In contrast, the AM1-CISD calculation gives a much smaller shift for **3** [$\Delta\tilde{\nu}$(MeCN–ether)$_{AM1} = -130$ cm^{-1}] than the experimental one [$\Delta\tilde{\nu}$(MeCN–ether)$_{exp} = -790$ cm^{-1}]. The discrepancy between experimental and computed solvent dependency of $\tilde{\nu}_{max}$ of **3** supports the assumption that the excitation of **3** is either localised intrinsically or by solvent induced symmetry breaking because these effects cannot be simulated by CI-calculations. This is due to the fact that in a CI-calculation all Franck–Condon excited states must belong to one of the irreducible representations of the point group of the ground state (approximate D_3 in the case of **3**). This shows that (in contrast to common belief) branched symmetric molecules without a permanent ground state dipole moment can show pronounced solvatochromism. The solvatochromic behaviour of **2** and **2-OMe** is reproduced well by the AM1-CI calculations. However, the computed solvatochromism is somewhat stronger for the z-polarised band than for the y-band, whereas the opposite trend is found experimentally. This effect overestimates the computational coupling energies derived from state splittings in the gas phase and leads to too small couplings in MeCN compared to the experimental band splittings (see Table 2).

Provided that the orbitals of the subchromophore branches overlap only weakly, exciton coupling theory[11] can be used to elucidate the electronic coupling of transition moments $\mu^{(p)}$ and $\mu^{(q)}$ localised at the centres p and q. Assuming D_3 symmetry for **3**, the interaction of the phenyl branches can be described by a 3 × 3 matrix [eqn. (1)], where V_{pq} is the coupling integral

$$\begin{vmatrix} E_a - E & V_{12} & V_{12} \\ V_{12} & E_a - E & V_{12} \\ V_{12} & V_{12} & E_a - E \end{vmatrix} = 0 \qquad (1)$$

between centres p and q which can be approximated by the point-dipole–point-dipole model [eqn. (2)].[11c]

$$V_{pq} = \mu_{0a}^{(p)}\mu_{0a}^{(q)}R_{pq}^{-3}\{e_p e_q - 3(e_p e_{pq})(e_q e_{pq})\} \qquad (2)$$

The transition moments μ_{0a} were calculated as one-third of the oscillator strength $f = 4.702 \times 10^{-7}\ \tilde{\nu}\mu_{0a}^2$ of **3**, the distance R_{pq} of the centres of the transition moments was calculated as the distance between the midpoints of two N(centre)–N(CN) distances of an AM1 optimised geometry (7.9 Å). e_p, e_q, and e_{pq} denote the unit vectors of $\mu^{(p)}$, $\mu^{(q)}$, and R_{pq}, respectively. By this method V was calculated to be 610 cm^{-1} which is in qualitative agreement with the AM1 calculated LUMO splitting energy (411 cm^{-1}, see Table 2). The same value is analogously obtained for **2**. Although the use of exciton coupling can be questioned in the present case because of orbital overlap of the phenyl branches with the central nitrogen, the results are in reasonable agreement with those of other methods (Table 2). This justifies the application of exciton coupling theory and proves **2** and **3** to be in the weak interaction regime.

Table 3 Experimental (HRS in MeCN), theoretical (tensor addition), and computed (AM1 TDHF, gas phase) static quadratic hyperpolarisabilities $\beta_{zzz(yyy)}$ (10^{-30} esu) of **1** and **3**. Values in parentheses are relative values

	HRS	Theor.	AM1-TDHF	β_{HRS}/M [a]
1	121		23.0	0.349
	(1)	(1)	(1)	
3	114		13.2	0.208
	(0.94)	(0.75)	(0.57)	
pTCVDA [b]	33			0.149

[a] $\beta_{zzz(yyy)}$ divided by the molecular mass (10^{-30} esu g^{-1} mol). [b] *p*-(Tricyanovinyl)-*N*,*N*-dimethylaniline, electric field induced second-harmonic generation (EFISH) measurement in CH_2Cl_2. λ_{max} (dioxane) = 516 nm,[26] λ_{max}(acetone) = 514 nm.[15]

C. Nonlinear optical properties

Subchromophore interactions can also be studied by measuring the quadratic hyperpolarisability. According to tensor addition calculations, the $\beta_{xxy} = -\beta_{yyy}$ value of a D_3 symmetric molecule should be 3/4 of the β_{zzz} value of its one-dimensional analogue if subchromophore interactions are negligible.[8a,21] For this reason, the quadratic hyperpolarisabilities β of **1** and **3** were measured by the hyper-Rayleigh scattering (HRS) technique[13] in MeCN (in this solvent the compounds investigated show no fluorescence at room temperature) which allows the determination of β for compounds with a zero ground state dipole moment. The 1500 nm laser output of an optical parametric power oscillator (OPPO) was used to avoid problems with two- and three-photon induced fluorescence as well as with resonantly enhanced second-harmonic generation light (SHG).[22] The unpolarised SHG signal was detected and compared to dimethylaminocinnamaldehyde as an external standard. Static hyperpolarisabilities were calculated by the two- and three-level approximation, respectively. Thus, for **1** $\beta^0_{zzz} = 121 \times 10^{-30}$ esu ($\beta^{1500}_{zzz} = 260 \times 10^{-30}$ esu) and for **3** $\beta^0_{yyy} = 114 \times 10^{-30}$ esu ($\beta^{1500}_{yyy} = 252 \times 10^{-30}$ esu) were obtained (see Table 3); this corresponds to a β_{yyy}:β_{zzz} ratio of 0.94. Provided that the subchromophores do not interact in **3**, the β_{yyy} element of **3** can be constructed by tensor addition from the β_{zzz} of **1**, if D_3 symmetry is assumed for **3**. By this method, a ratio of 0.75 is expected. AM1 time-dependent Hartree–Fock (TDHF) calculations[23] yield an even smaller ratio of 0.57 (see Table 3).

The quadratic hyperpolarisability of a D_3 symmetric molecule can be approximated by a three-level model [eqn. (3)],[24]

$$\beta_{yyy} = \frac{1}{\hbar^2} \times \frac{{\mu_{01}}^2\mu_{12}}{{\omega_{01}}^2} \times \frac{{\omega_{01}}^4}{({\omega_{01}}^2 - 4\omega^2)({\omega_{01}}^2 - \omega^2)} \qquad (3)$$

where ${\mu_{01}}^2$ denotes the square of the transition moment between ground and degenerate first excited CT states, μ_{12} is the transition moment connecting these degenerate excited states, ω_{01} is the CT energy, and ω is the fundamental laser energy of the HRS experiment.

Since the CT energy is almost the same for **1** and **3** and the oscillator strength, which is proportional to the square of the transition moment μ_{01}, is even smaller for **3** than for **1** as expected from the 3:1 ratio, the experimental β_{yyy}:β_{zzz} ratio of

Table 4 Redox potentials of **1**–**3** [*E*/mV] *vs*. ferrocene (Fc/Fc^+) in MeCN

	M^+/M	M/M^-	M^-/M^{2-}	M^{2-}/M^{3-}
1	870[a]	−960		
2	1055[a]	−800	−970	
2-OMe	825	−795	−970	
3	1240	−700[b]		−885

[a] Irreversible process, peak potential. [b] Unresolved two electron process.

0.94 compared to 0.75 or even more to 0.57 suggests that transition moment μ_{12} connecting the excited states is higher than one would have assumed by a simple additivity model. This behaviour has been found for several two- and three-dimensional NLO chromophores where β_{yyy} of the octupolar chromophore is enhanced compared to β_{zzz} of the 1D reference system.[25] Although this type of coupling cannot be measured in energy terms it proves a certain coupling of subchromophore units in the excited states of **3**.

In Table 3, $\beta_{yyy}(\beta_{zzz})$ divided by the molecular mass is given together with the values for *p*-(tricyanovinyl)-*N*,*N*-dimethylaniline. Comparison of these values shows that the triarylamine derivatives perform much better than the chromophore with the dialkylamino donor at practically no cost of transparency.[26] This might be due to the higher polarisability of a diphenylamino group compared to a dialkylamino group as found theoretically by McMahon *et al*.[27] Moylan *et al*.[28] investigated a number of one-dimensional NLO-chomophores with dialkylamino or diarylamino donor substituents combined with various acceptor units. In those cases where the π-electron system is a tolane, stilbene or an even larger system, the difference between the diphenylamino and the dialkylamino groups concerning the quadratic hyperpolarisability is marginal. However, in cases where the π-electron system is small (*e.g*. a phenyl group), the β values of the diarylamino compounds are more than twice that of the dialkylamino derivatives. This suggests that the intrinsically larger polarisability of a triarylamine functionality has its highest influence in small compounds where it contributes the major part of the π-electron system.

D. Redox properties

Electronic coupling of charged ground state species can be measured by their redox potentials. Accordingly, cyclic voltammograms of compounds **1**–**3** have been measured in MeCN. Compounds **2-OMe** and **3** show reversible oxidative steps for the amine oxidation, whereas the oxidation of **1** and **2** is irreversible due to the unprotected *para*-position of the phenyl groups. The derivatives **1**–**3** show waves corresponding to reversible reduction processes of the respective number of tricyanovinyl groups (Table 4 and Fig. 3). For **3**, the first two reductions are close in potential and merge into one unresolved wave. The redox potentials correspond approximately to the LUMO energies in the Hückel-type orbital diagram (Scheme 2). Thus, for **2** and **2-OMe** a splitting is observed which is twice the electronic coupling V and for **3**, two almost degenerate steps (corresponding to the orthogonal e-type LUMOs) and one step at more negative potential (a-type LUMO) are present. The potential difference between the "two electron process" and the one electron reduction corresponds to $3 \times V$. Coupling energies derived by this method are given in Table 2. However, it must be stressed that this correlation is very approximate and refers to charged species, *i.e*. the redox potential difference in **3** mirrors the electronic coupling of a species which has two negative charges and which is compared to a species with three negative charges. Therefore, these values must be interpreted cautiously and cannot be directly compared to the electronic coupling in the corresponding neutral system. Nonetheless, the correspondence to the orbital diagram (Scheme 2) is close as the interactions between the branches are weak.

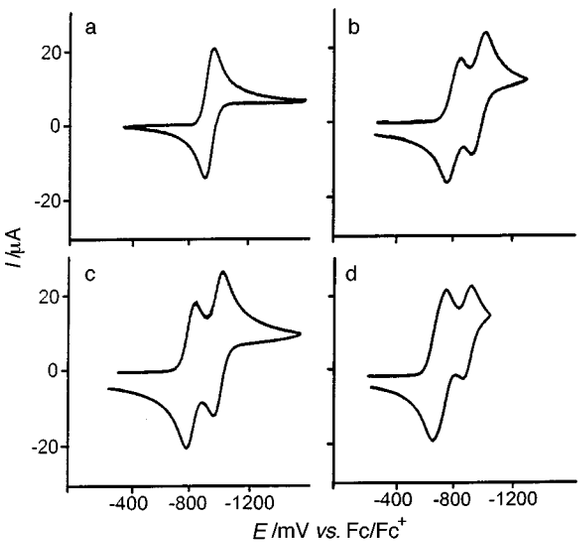

Fig. 3 Cyclic voltammograms of **1**–**3** in MeCN *vs*. ferrocene (Fc/Fc^+): a) **1**, b) **2**, c) **2-OMe**, d) **3**.

In order to obtain structural and electron distribution information about the charged species, we performed AM1 calculations. The unrestricted Hartree–Fock (UHF) optimised structures of compounds $\mathbf{2}^-$, $\mathbf{2\text{-}OMe}^-$, $\mathbf{3}^-$, $\mathbf{3}^{2-}$, $\mathbf{3}^{3-}$ together with the neutral compounds **2-OMe** and **3** are displayed in Schemes 3 and 4. The Coulson charge distributions are grouped together for the central amine nitrogen, the phenyl groups and the tricyanovinyl moieties and refer to CI calculations on the UHF optimised geometries (see Experimental section). As expected, all molecules show a propeller-like geometry in the neutral state. The dihedral angles of the phenyl ring planes with the central plane, formed by the amine nitrogen and the three adjacent carbon atoms [$N(C)_3$] are *ca*. 30–34°. The methoxy derivative **2-OMe** differs in that the methoxyphenyl moiety is somewhat more turned out of the central plane (by *ca*. 56°).

In the monoanion $\mathbf{3}^-$, the charge is localised at the tricyanovinyl moiety of a single branch. This branch is turned out of the central plane by 51° in order to minimise electronic repulsion between the extra charge and the central nitrogen lone pair electrons. The N(amine)–C bond of this branch is somewhat elongated (1.426 Å) compared to the other C–N bonds (1.402 Å). In the dianion $\mathbf{3}^{2-}$, the two negative charges formally occupy the e-type orbitals (Scheme 2) and are localised in two subchromophore branches. Again, these branches are twisted out of the $N(C)_3$ plane (51°); however, the third (neutral) branch has a reduced dihedral angle of 13°. At the same time, the N–C(phenyl) distance of the neutral tricyanovinylphenyl group is significantly shorter (1.379 Å) than those of the charged branches (1.424 Å). In this way, a cross conjugated system is formed (see Scheme 3) where the radical centres avoid conjugation with each other (see Scheme 5). This is a consequence of the strong TCV-acceptor functionality in the third (neutral) phenyl branch. Similar bond localisations were discussed for a tri(*N*-*tert*-butyl-*N*-oxyaminophenyl)methyl diradical.[29] Interestingly, the CI calculation for $\mathbf{3}^{2-}$ suggests a triplet ground state to be 0.62 kcal mol^{-1} more stable than a singlet ground state. Although the low-lying triplet state might be an artifact due to "triplet instability",[30] the fact that the singlet–triplet splitting is small supports the interpretation that the coupling (and, hence, the electrostatic repulsion) between the two charged branches is diminished by forming a cross conjugated system. On the other hand, the coupling between the charged and the neutral tricyanovinylphenyl ring is enhanced, which can be seen by an IV-CT band in the NIR (see below). Due to this enhancement, the third electron entering the system

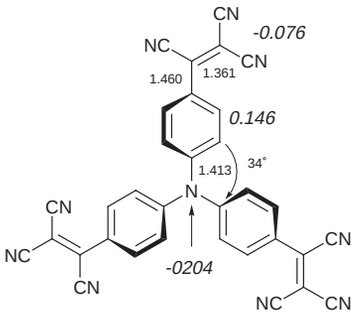

^{1}[3]

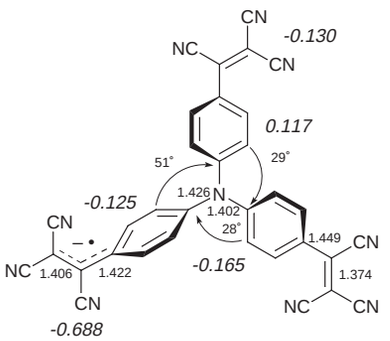

^{2}[3$^-$]

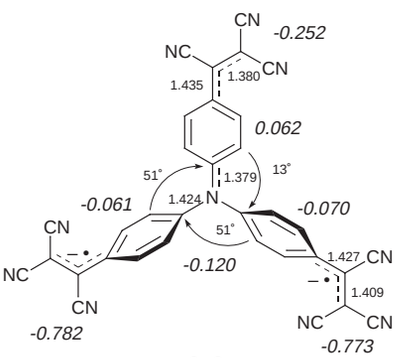

^{3}[3^{2-}]

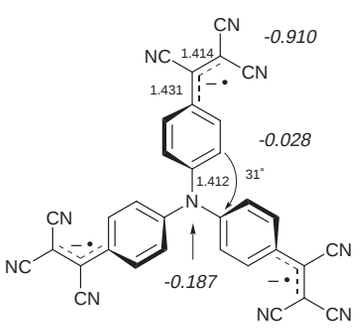

^{2}[3^{3-}]

Scheme 3

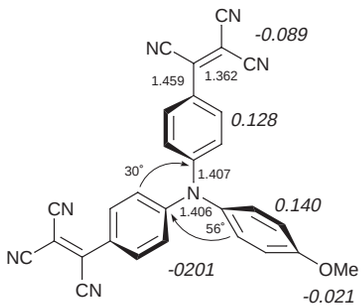

^{1}[2–OMe]

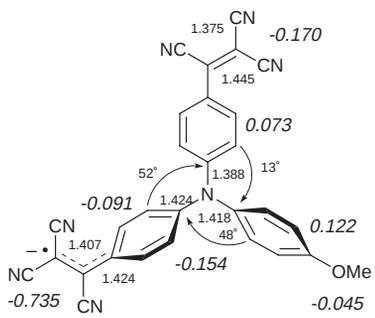

^{2}[2–OMe$^-$]

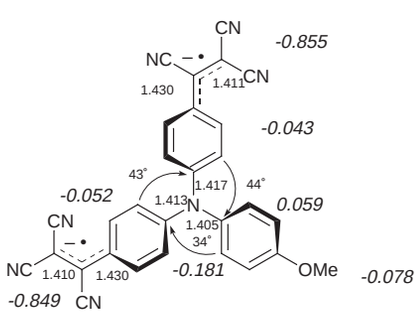

^{1}[2–OMe^{2-}]

Scheme 4

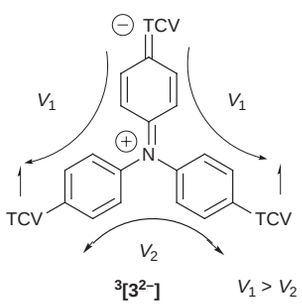

Scheme 5

in order to form the trianion interacts more strongly with the two negatively charged branches. By charging the third branch the cross conjugation is destroyed (see Scheme 3). This leads to spin pairing of the third electron which results in a doublet trianion rather than in a quartet state ($\Delta E_{D\text{-}Q} = -0.43$ kcal mol^{-1}).[31] The trianion has a symmetric structure and resembles the neutral species. However, the vinyl C=C distances of **3**$^{3-}$ (and of **3**$^-$ and **3**$^{2-}$) are somewhat elongated (1.414 Å) compared to **3** (1.361 Å). Although the singlet–triplet and doublet–quartet splitting energies are very small, and both spin states might be populated thermally at room temperature, our computational observation that **3**$^{2-}$ is a triplet ground state due to a cross conjugated system and that the trianion is a doublet ground state because of spin pairing is in line with calculations by Lahti and Ichimura.[32] These authors observed triplet ground states for similar cross conjugated systems and singlet ground states for analogous systems where cross conjugation is destroyed by a nitrogen with a lone pair. The spin pairing situation in **3**$^{2-}$ and **3**$^{3-}$ is sketched in Schemes 5 and 6.

The geometry and electronic structure of the monoanion **2-OMe**$^-$ is similar to the dianion **3**$^{2-}$ where one anionic tricyanovinylphenyl group is replaced by a methoxyphenyl group. The extra charge is localised in one branch. This branch and the methoxyphenyl group are strongly twisted out of the N(C)$_3$ plane (48° and 52°) as in **3**$^{2-}$. The neutral branch has a reduced N–C bond length (1.388 Å); again a cross conjugated system is formed, reducing the interaction between the charged branch and the methoxyphenyl group and enhancing the coupling

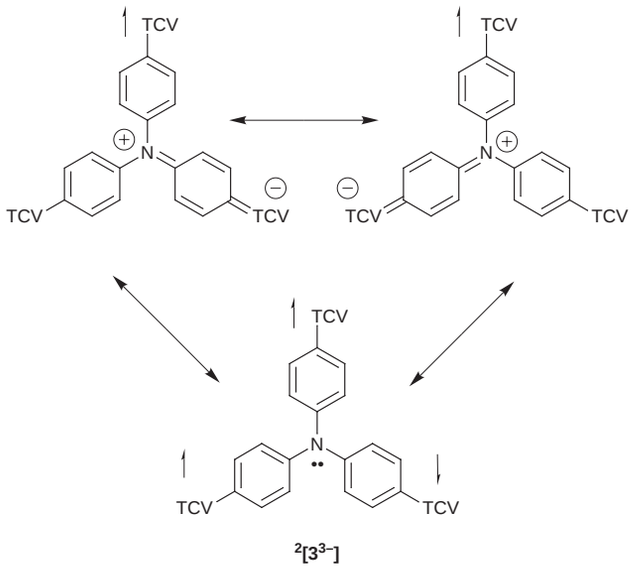

Scheme 6

between the charged and the neutral tricyanovinylphenyl moieties. The dianions $\mathbf{2}^{2-}$ and $\mathbf{2\text{-}OMe}^{2-}$ resemble $\mathbf{3}^{3-}$, the cross conjugation is destroyed and the geometry is more symmetric. The electronic (charge populations) and geometrical structures of **2**, $\mathbf{2}^{-}$, and $\mathbf{2}^{2-}$ deviate only marginally from the ones of their methoxy substituted counterparts; the only difference is the unsubstituted phenyl group which is less twisted out of the central plane (*ca.* 43° in **2**, 39° in $\mathbf{2}^{-}$, and 29° in $\mathbf{2}^{2-}$). For this reason, pictures are omitted here. CI calculations suggest the singlet state to be slightly more stable than the triplet state for $\mathbf{2}^{2-}$ ($\Delta E_{S-T} = -0.11$ kcal mol^{-1}) and $\mathbf{2\text{-}OMe}^{2-}$ ($\Delta E_{S-T} = -0.10$ kcal mol^{-1}). This shows that the coupling between the charged centres in $\mathbf{2\text{-}OMe}^{2-}$ and $\mathbf{2}^{2-}$ is somewhat stronger than in $\mathbf{3}^{2-}$ where the triplet state is the ground state.

The geometrical analysis nicely demonstrates that the doubly charged [or singly charged and one donor (methoxy) group] triphenylamines reduce destabilising electrostatic repulsion by cross conjugation. This geometrical consequence should lead to two different coupling interactions in the charged species where $V_1 > V_2$ (Scheme 5).

E. UV-Vis-NIR-Spectroelectrochemistry

The UV-Vis-NIR spectra of the negatively charged species formed during electrochemical reduction of **1**–**3** were recorded in transmission in a thin-layer cell in MeCN solutions. These spectra are mainly characterised by a decrease of the CT band intensity at *ca.* 500 nm and the increase of a weak band at *ca.* 670 nm. For compound **2** and **2-OMe**, a low intensity band in the NIR at 1080 nm (9250 cm^{-1}) and at 1150 nm (8700 cm^{-1}), respectively, rises upon reduction to $\mathbf{2}^{-}$ or $\mathbf{2\text{-}OMe}^{-}$ which we assign to an intervalence charge transfer (IV-CT) band of the monoradical anion $\mathbf{2}^{-}$ ($\mathbf{2\text{-}OMe}^{-}$) (see Fig. 4). This band refers to a degenerate photoinduced intramolecular electron transfer (ET) from a negatively charged tricyanovinyl moiety to a neutral one (see Scheme 7).[20,33] Upon reduction to the dianion, this IV-CT band disappears. In principal, both the monoanion and the dianion of **3** could display an IV-CT band (see Scheme 7). Actually, such a band is only observed in $\mathbf{3}^{2-}$ at 1190 nm. This band disappears when $\mathbf{3}^{2-}$ is reduced to the trianion $\mathbf{3}^{3-}$. The coupling in the monoanion of **3** is too weak to be observable, which is due to the orthogonal character of the degenerate e-type LUMOs in **3** (one of those is singly occupied in $\mathbf{3}^{-}$, see Scheme 2), as can also be seen by the small redox potential separation between $\mathbf{3}^{-}$ and $\mathbf{3}^{2-}$ (the actually unresolved process in the CV, see Fig. 3d). The IV-CT character of the observed bands is supported by the fact that the experimental band width

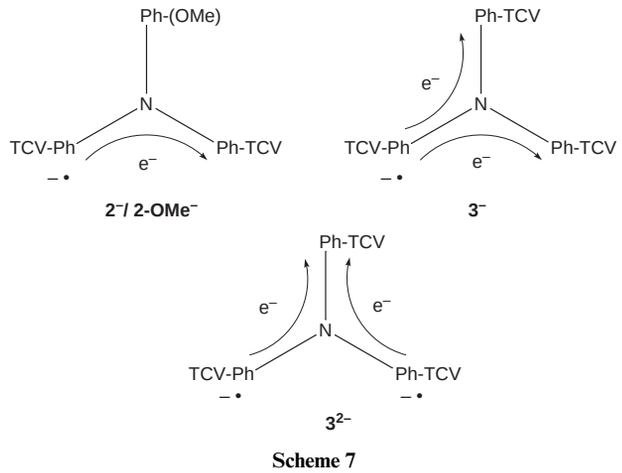

Scheme 7

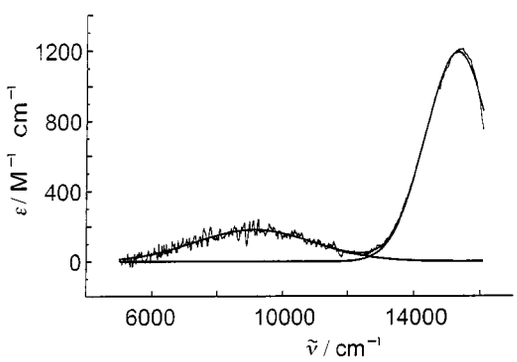

Fig. 4 IV-CT band of $\mathbf{2}^{-}$ in the NIR from the spectroelectrochemical experiment and Gaussian curve fits.

at half-height is slightly (*ca.* 5–10%) broader than the theoretical band width at the high-temperature limit [$\tilde{\nu}_{1/2}$(HTL) = $47.94\sqrt{\tilde{\nu}_{max}}$].[12b]

According to Hush,[12] the electronic coupling can be calculated from the band shape analysis of the IV-CT band using eqn. (4). In this equation, d is the distance between the charged

$$V = \frac{0.0206}{sd}(\varepsilon_{max}\tilde{\nu}_{1/2}\tilde{\nu}_{max})^{1/2} \qquad (4)$$

centres [we used the AM1 calculated distance between the first vinyl C atom of the tricyanovinyl groups (11.5 Å)],[34] ε_{max} is the molar absorptivity of the IV-CT band,[35] $\tilde{\nu}_{max}$ the band energy and $\tilde{\nu}_{1/2}$ the band width at half-height. s is a symmetry factor which is 1 in a one-dimensional system and $2^{1/2}$ in a two-dimensional ET system.[20] It must be stressed that this method only gives an averaged coupling for the two-dimensional system $\mathbf{3}^{2-}$. Due to the deviation from D_3 symmetry, there are actually two different couplings (see AM1 calculations below and Scheme 5).

With the data from Table 5 a somewhat higher coupling energy (310 cm^{-1}) is calculated for $\mathbf{2\text{-}OMe}^{-}$ than for $\mathbf{2}^{-}$ (170 cm^{-1}) and for $\mathbf{3}^{2-}$ (160 cm^{-1}) (see Table 2). This is due to the methoxy donor substituent in **2**, which enlarges the splitting of the LUMOs owing to a destabilising interaction with the a-type LUMO (see Scheme 2). This demonstrates that the extent of coupling between two tricyanovinylphenyl (TCV-phenyl) groups can be governed by the third amine substituent:

TCV-phenyl < [TCV-phenyl]$^{\bullet -}$ < phenyl < MeO-phenyl
$\mathbf{3}^{-}$ $\mathbf{3}^{2-}$ $\mathbf{2}^{-}$ $\mathbf{2\text{-}OMe}^{-}$
$\longrightarrow$ increasing coupling $\longrightarrow$

In addition, the coupling strength can be reversibly switched between $\mathbf{3}^{-}$ and $\mathbf{3}^{2-}$ by electrochemical methods.

Table 5 Optical data of the IV-CT bands of $\mathbf{2}^-$, **2-OMe**$^-$ and $\mathbf{3}^{2-}$

	$\tilde{\nu}_{max}$/cm^{-1} = λ/kcal mol^{-1} [a]	λ_v/kcal mol^{-1} [b]	$\tilde{\nu}_{1/2}$/ cm^{-1} [c]	$\tilde{\nu}_{1/2}$(HTL)/ cm^{-1} [d]	ε_{max}/ M^{-1} cm^{-1} [e]	V/cm^{-1} [f]
2-OMe$^-$	8700(24.9)	10.9	4850	4470	650	310
$\mathbf{2}^-$	9250(26.4)		4720	4610	205	170
$\mathbf{3}^{2-}$	8400(24.0)	7.2	4600	4390	420	160

[a] IV-CT energy. [b] AM1 calculated internal reorganisation energy. [c] Experimental band width at half-height. [d] Theoretical band width at half-height at high temperature limit. [e] Molar absorptivity. [f] Electronic coupling energy.

The coupling energies of $\mathbf{2}^-$, **2-OMe**$^-$, and $\mathbf{3}^{2-}$ are in the same order as those of the radical cations of *meta*-phenylene connected triarylamines (*ca.* 200–400 cm^{-1}).[33d] Again, the electronic coupling evaluated by Hush analysis refers to charged species and cannot directly be compared to the coupling in the neutral systems of **2**, **2-OMe** and **3**.

The $\tilde{\nu}_{max}$ of the IV-CT bands corresponds to the Marcus reorganisation energy λ. The internal (vibrational) contribution to λ can be estimated with the method by Nelsen *et al.* [eqn. (5)][36] where n^0 is the AM1 calculated heat of formation of the

$$\lambda_v = n^- - a^- + a^0 - n^0 \quad (5)$$

neutral molecule in the geometry of the neutral molecule, n^- is the UHF calculated heat of formation of the anion in the neutral geometry, and a^0 and a^- are the respective values for the anion geometry.

This gives 10.9 kcal mol^{-1} for the internal reorganisation energy of **2-OMe**/**2-OMe**$^-$, 11.3 kcal mol^{-1} for **3**/**3**$^-$ and 7.2 kcal mol^{-1} for $\mathbf{3}^-/\mathbf{3}^{2-}$ which is about 1/3 to 1/4 of the total reorganisation energy (see Table 5). The internal contributions λ_v are higher than in triarylamine radical cation systems (λ_v *ca.* 4–5 kcal mol^{-1})[37] because of stronger angle distortions (twisting of the phenyl groups) and, even more pronounced, stronger bond distance distortions [N(amine)–C bonds, vinyl group] during the IV-CT process.

The internal reorganisation energy can be used to estimate V by eqn. (6)[38] in the gas phase where $\lambda = \lambda_v$. In this equation,

$$\Delta G_{res} = \frac{V^2}{\lambda} \quad (6)$$

ΔG_{res} is the resonance energy, *i.e.*, the energy by which the system is stabilised in the ground state due to resonance interaction of the localised radical centre with the coupling acceptor functionalities. ΔG_{res} can be approximately calculated by eqn. (7) where we used AM1-RHF energies for **1** and **3** and RHF

$$\Delta G_{res} \approx \Delta H_{res} = \Delta H_f(\mathbf{1}) + \Delta H_f(\mathbf{3}^-) - \Delta H_f(\mathbf{3}) - \Delta H_f(\mathbf{1}^-) \quad (7)$$

single point energies (half electron formalism) on UHF optimised structures for $\mathbf{1}^-$ and $\mathbf{3}^-$.

From eqn. (7), ΔG_{res} of −2.82 kcal mol^{-1} is obtained which refers to V = 1974 cm^{-1}. As this value involves the coupling to two equivalent sites it must be divided by the symmetry factor $2^{1/2}$ which then gives an averaged coupling of V = 1396 cm^{-1}. Although this value is in good agreement with coupling energies estimated for neutral **3** (see Table 2), it is much too high compared to the 160 cm^{-1} value calculated from the Hush analysis for $\mathbf{3}^-$.

By using AM1-CI calculations the IV-CT band energies were computed for $\mathbf{2}^-$, **2-OMe**$^-$, **3-**, and $\mathbf{3}^{2-}$ (see Table 6). Although the calculated energies are in good agreement with the experiment (see Table 2), this is certainly fortuitous because the AM1 calculations refer to the gas phase and, accordingly, the IV-CT energies correspond to the internal reorganisation energy λ_v which should be much smaller than the experimentally observed total reorganisation energy. For $\mathbf{3}^-$ and $\mathbf{3}^{2-}$, there are two IV-CT bands which are orthogonally polarised and too close in energy to be resolved experimentally as two bands. From the AM1 transition energies and the oscillator strengths we calculated the electronic coupling energies V *via* eqn. (4) and $\varepsilon\tilde{\nu}_{1/2} = (2.315 \times 10^8) f$. The coupling energies are significantly too high compared to the experimental Hush values, due to the overemphasised IV-CT energies. Nonetheless, one can draw some conclusions: Again, the methoxy derivative **2-OMe**$^-$ shows a somewhat higher coupling than $\mathbf{2}^-$. Anions $\mathbf{3}^-$ and $\mathbf{3}^{2-}$ have two coupling energies associated with the two perpendicular IV-CT transitions. They reflect the different degree of coupling between the neutral and the charged branches on one hand (strong coupling) and between two charged (neutral) branches (weak coupling) in $\mathbf{3}^{2-}$ and $\mathbf{3}^-$ on the other hand (see Schemes 5 and 7). Although the qualitative couplings can be deduced very well by AM1-CI calculations, a quantitative evaluation is hampered owing to the CI expansions used being far beyond a converged limit.

Table 6 AM1-CI calculated IV-CT band energies and coupling energies

	$\tilde{\nu}_{max}$/cm^{-1} [a]	f [b]	V/cm^{-1} [c]
$\mathbf{2}^-$	7079	0.326	1310
2-OMe$^-$	7061	0.523	1660
$\mathbf{3}^-$	6315	0.024	370*y*
	8380	0.548	1850*z*
$\mathbf{3}^{2-}$	7344	0.397	1470*z*
	9641	0.011	280*y*

[a] IV-CT energy. [b] Oscillator strength. [c] Electronic coupling energies. The *y* axis is along the negatively charged phenly group in $\mathbf{3}^-$ and along the neutral phenyl group in $\mathbf{3}^{2-}$.

Conclusions

The different experimental and theoretical methods employed yield coupling energies for **2** and **3** in the order of 200–1700 cm^{-1}. The coupling energies derived from the UV-band splittings, the exciton coupling theory and the AM1-CI state splittings in the gas phase (Table 2) refer to neutral systems and give values between *ca.* 600–1700 cm^{-1} for **2** and **2-OMe** and 600–1200 cm^{-1} for **3**. Hush's band shape analysis has been used to deduce coupling energies from the IV-CT bands of radical anions $\mathbf{2}^-$, **2-OMe**$^-$ and $\mathbf{3}^{2-}$. This is, besides the system described by Bonvoisin *et al.*[33e] the only other case known to us where IV-CT bands were observed and appropriately interpreted in purely organic radical anions. The coupling energies from the cyclic voltammograms and the Hush analysis of IV-CT bands refer to charged species and give much smaller values of 160–500 cm^{-1} for $\mathbf{3}^{2-}$ and 170–700 cm^{-1} for $\mathbf{2}^-$ and **2-OMe**$^-$. All methods show that the coupling in **2-OMe**$^-$ is stronger than in $\mathbf{2}^-$ and that the coupling in $\mathbf{2}^-$ and $\mathbf{3}^{2-}$ is larger than in $\mathbf{3}^-$. Thus, the degree of coupling between two TCV-phenyl groups can be influenced by the third amine substituent. The overall coupling in the acceptor substituted triarylamines is small as can be seen from the small coupling energies compared to the total reorganisation energy of $\mathbf{2}^-$ and $\mathbf{3}^{2-}$.

The solvent dependent absorption spectra of **3** support an excitation intrinsically localised within one branch. This is in line with the coupling energy V being much smaller than the band width. The weak subchromophore interaction is to some extent due to the propeller-like geometry. But as interaction integrals vary approximately as a cos function, the interaction at a dihedral angle of *ca*. 30° is still 80–90%. The main reason for the weak interaction is the fact that the tricyanovinyl groups are extremely strong acceptor groups. The LUMO orbital coefficients are practically localised at the tricyanovinyl groups. One expects stronger interactions in substituted triarylamines with weaker acceptor functionalities where stronger LUMO orbital overlap is present. This is indeed observed in the formyl substituted triarylamines. For example, di(4-formylphenyl)phenylamine has a coupling energy of 2300 cm^{-1} from UV-Vis band splitting, which is larger than half the band width[19] (see Table 2).

Cyclic voltammetry and AM1-CI calculations show that electrons added by reduction are localised in single branches and lead to structural distortions (mainly rotation of the phenyl groups). The small coupling leads to the preferred triplet state of $\mathbf{3}^{2-}$. The spin state in this system can be switched electrochemically from singlet (**3**)→doublet ($\mathbf{3}^{-}$)→triplet ($\mathbf{3}^{2-}$)→doublet ($\mathbf{3}^{3-}$).

Despite weak interactions in the ground state, the HRS measurements together with the TDHF calculations prove that there are excited state couplings in **3** which lead to an enhanced quadratic hyperpolarisability of **3** compared to the 1D analogue **1**. In contrast, **1** and **3** differ only marginally in their absorption maxima. The β-value of **1** is much higher than in an analogous dialkylamino derivative which is due to the intrinsically higher polarisability of a triarylamine compared to a dialkylaniline.

Experimental

Syntheses

Commercial grade reagents were used without further purification. Solvents were purified, dried, and degassed following standard procedures. Syntheses of di(4-formylphenyl)phenylamine[39] and di(4-formylphenyl)methoxyphenylamine[2a,39] have been reported previously. Tri(4-formylphenyl)amine was synthesised from tri(4-lithiophenyl)amine and DMF.[2a]

4-(Tricyanovinyl)phenyl(diphenyl)amine 1. Tetracyanoethylene (384 mg 3.00 mmol) was added to a solution of triphenylamine (630 mg, 2.57 mmol) in 10 ml of absolute DMF. The dark violet solution was stirred for 14 hours at room temperature. The solution was poured onto ice (100 g) and the resulting solid was suction filtered and washed with water (3 × 10 ml). Chromatography (SiO_2, CH_2Cl_2) afforded 630 mg of **1** (71%) as dark violet crystals, mp 181 °C (Found: C, 79.7; H, 4.4; N, 16.5. Calc. for $C_{23}H_{14}N_4$: C, 79.75; H, 4.1; N, 16.2%); ν_{max}(KBr)/cm^{-1} 2220 (CN); δ_H(250 MHz; $CDCl_3$) 7.98 (2H, m, AA′, phenylene H), 7.27 (10 H, m, phenyl H), 6.94 (m, BB′, 2 H, phenylene H); δ_C(62.9 MHz; $CDCl_3$) 154.6, 144.3, 138.2, 132.2, 130.2, 127.1, 127.0, 120.2, 118.0, 114.2, 113.2, 113.0, 81.9; *m/z* 346 (M^+, 100%), 321 ($M^+ - CN + H$, 17).

Tris[4-(2,2-dicyanovinyl)phenyl]amine. To a solution of tri(4-formylphenyl)amine (140 mg, 0.42 mmol) in 15 ml of anhydrous pyridine, 1 g molecular sieves (3 Å), one crystal of ammonium acetate, 5 drops of acetic acid and 100 mg (1.52 mmol) of malonodinitrile were added. The reaction mixture was stirred at RT and monitored by TLC. After 2 h the pyridine was removed under reduced pressure and the residue dissolved in CH_2Cl_2. The organic layer was washed with water (3 × 20 ml) and dried over Na_2SO_4. Chromatography (SiO_2, CH_2Cl_2–ethyl acetate 9 : 1) and recrystallisation from CH_2Cl_2–hexane afforded 183 mg (92%) of orange crystals, mp 192–193 °C (Found: C, 75.8; H, 3.5; N, 20.55. Calc. for $C_{30}H_{15}N_7$: C, 76.1; H, 3.2; N, 20.7%); ν_{max}(KBr)/cm^{-1} 2225 (CN); δ_H(250 MHz, [D_6]DMSO) 8.46 (1 H, s, olefinic H), 7.99 (2 H, m, AA′, H-3), 7.34 (2 H, m, BB′, H-2); δ_C(62.9 MHz, [D_6]DMSO) 159.7, 149.9, 132.8, 127.6, 124.8, 114.5, 113.5, 79.1; *m/z* 473 (M^+, 100%), 448 ($M^+ - CN + H$, 4), 410 [$M^+ - C(CN)_2 + H$, 10].

Bis[4-(2,2-dicyanovinyl)phenyl]phenylamine. This compound was prepared analogously to tris[4-(2,2-dicyanovinyl)phenyl]amine from di(4-formylphenyl)phenylamine. Chromatography (SiO_2, CH_2Cl_2–hexane 4 : 1) and recrystallisation from CH_2Cl_2–hexane gave 740 mg (80%) of orange crystals, mp 228–232 °C; ν_{max}(KBr)/cm^{-1} 2225 (CN); δ_H(400 MHz, [D_6]DMSO) 8.36 (2 H, s, olefinic H), 7.83 (4 H, m, AA′, phenylene H), 7.48 (2 H, m, phenyl H), 7.35 (1 H, m, phenyl H), 7.22 (2 H, m, phenyl H), 7.18 (4 H, m, BB′, phenylene H); δ_C(100.6 MHz, [D_6]DMSO) 159.6, 150.8, 144.2, 132.7, 130.5, 127.4, 127.1, 125.9, 122.5, 114.8, 113.8, 77.4; *m/z* 397 (M^+, 100%), 372 ($M^+ - CN + H$, 3), 334 [$M^+ - C(CN)_2 + H$, 4]; MS (EI, 70 eV, high resolution): *m/z* found: 397.1329, calc. for $C_{26}H_{15}N_5$: 397.1328.

Bis[4-(2,2-dicyanovinyl)phenyl](4′-methoxyphenyl)amine. This compound was prepared analogously to tris[4-(2,2-dicyanovinyl)phenyl]amine from di(4-formylphenyl)(4′-methoxyphenyl)amine. Chromatography (SiO_2, CH_2Cl_2) and recrystallisation from CH_2Cl_2–hexane gave 345 mg (84%) of orange crystals, mp 167–171 °C (Found: C, 75.6; H, 4.4; N, 16.0. Calc. for $C_{27}H_{17}N_5O$: C, 75.9; H, 4.0; N, 16.4%); ν_{max}(KBr)/cm^{-1} 2225 CN); δ_H(400 MHz, [D_6]acetone) 8.15 (2 H, s, olefinic H), 8.00 (4 H, m, AA′, aromatic H), 7.23–7.29 (6 H, m, BB′, AA′, aromatic H), 7.08 (2 H, m, BB′, aromatic H), 3.87 (3 H, s, OCH_3); δ_C(100.6 MHz, [D_6]acetone) 159.8, 159.7, 152.4, 138.0, 133.6, 130.2, 126.8, 123.1, 116.5, 115.4, 114.5, 78.90, 55.9; *m/z* 427 (M^+, 100), 412 ($M^+ - OMe$, 44).

Tris[4-(tricyanovinyl)phenyl]amine 3. To a solution of tris[4-(2,2-dicyanovinyl)phenyl]amine (420 mg, 0.89 mmol) in 10 ml of DMF a solution of 212 mg (4.32 mmol) of NaCN in 2 ml of water–DMF (1 : 1 v/v) was added at 0 °C. The orange solution became colourless after complete addition. Acetic acid (5 drops) and 1 drop of conc. HCl were added, followed by lead tetraacetate (1200 mg, 2.70 mmol) in small portions. After stirring for 1 h at 0 °C, the dark violet solution was poured onto ice (100 g). The resulting solid was suction filtered and washed with water (3 × 10 ml). Flash chromatography (SiO_2, CH_2Cl_2) and recrystallisation from CH_2Cl_2–hexane afforded 100 mg (21%) of a violet powder, mp 178 °C; ν_{max}(KBr)/cm^{-1} 2232 (CN), 2224 (CN); δ_H(250 MHz, [D_6]acetone) 8.16 (6 H, m, AA′, H-3), 7.70 (6 H, m, BB′, H-2); δ_C(62.9 MHz, [D_6]acetone) 51.7, 140.7, 132.7, 126.6, 126.4, 115.0, 113.1, 112.7, 92.5; *m/z* 548 (M^+, 100%), 523 ($M^+ - CN + H$, 21); MS (EI, 70 eV, high resolution): *m/z* found: 548.1255, calc. for $C_{33}H_{12}N_{10}$: 548.1246.

Bis[4-(tricyanovinyl)phenyl]phenylamine 2. This compound was prepared analogously to tris[4-(tricyanovinyl)phenyl]amine (**3**) from bis[4-(2,2-dicyanovinyl)phenyl]phenylamine. Chromatography (SiO_2, CH_2Cl_2) and recrystallisation from CH_2Cl_2–hexane gave 408 mg (86%) of violet crystals, mp 251–252 °C (Found: C, 74.9; H, 3.2; N, 21.8. Calc. for $C_{28}H_{13}N_7$: C, 75.2; H, 2.9; N, 21.9%); ν_{max}(KBr)/cm^{-1} 2230 (sh), 2222 (CN); δ_H(400, MHz, $CDCl_3$) 8.04 (4 H, m, AA′, phenylene H), 7.51 (2 H, m, phenyl H), 7.42 (1 H, m, phenyl H), 7.26 (4 H, m, BB′, phenylene H), 7.21 (2 H, m, phenyl H); δ_C(100.6 MHz, $CDCl_3$) 51.8, 143.4, 139.1, 131.8, 130.9, 128.5, 127.6, 123.6, 123.0, 113.7, 111.9, 111.8, 88.1; *m/z* 447 (M^+, 100%), 422 ($M^+ - CN + H$, 10), 399 (4).

Bis[4-(tricyanovinyl)phenyl](4′-methoxyphenyl)amine 2-OMe. This compound was prepared analogously to tris[4-(tri-

cyanovinyl)phenyl]amine (**3**) from bis[4-(2,2-dicyanovinyl)-phenyl](4′-methoxyphenyl)amine. Chromatography (SiO_2, CH_2Cl_2) and recrystallisation from CH_2Cl_2–hexane gave 106 mg (85%) of violet crystals, mp 178–180 °C; ν_{max}(KBr)/cm^{-1} 2232 (sh), 2222 (CN); δ_H(400 MHz, $CDCl_3$) 8.04 (4 H, m, AA′, phenylene H), 7.25 (4 H, m, BB′, phenylene H), 7.13 (2 H, m, AA′, phenylene H), 7.02 (2 H, m, BB′, phenylene H), 3.88 (3 H, s, OCH_3); δ_C(100.6 MHz, $CDCl_3$) 159.5, 151.9, 139.0, 135.8, 131.8, 129.1, 123.4, 122.6, 116.1, 113.7, 112.0, 111.9, 87.6, 55.7; *m*/*z* 477 (M^+, 100), 462 (M^+ − OMe, 36); MS (EI, 70 eV, high resolution): *m*/*z* found: 477.1334, calc. for $C_{29}H_{15}N_7O$: 477.1338.

UV–Vis spectra

Spectra were recorded at ambient temperature in spectrograde solvents at 10^{-5}–10^{-6} M^{-1} concentrations. No deviations of Beer–Lambert's law were observed in this range.

HRS-Measurement

The experimental set-up is described in detail in ref. 22. Hyper-Rayleigh scattering measurements were done with solutions of **1** and **3** in MeCN at number densities between 0.20–3.44 × 10^{18} ml^{-1}. No fluorescence could be detected for MeCN solutions of **1** and **3**. Negative deviation of the HRS signal of **1** from linearity was observed above 3.44 × 10^{18} ml^{-1} due to self absorption of the SHG. Only those points obeying a linear correlation and the blank solvent signal were used for the data evaluation. *p*-Dimethylaminocinnamaldehyde (β_{zzz} = 58 × 10^{-30} esu at 1500 nm in MeCN)[40] was used as the reference under identical experimental conditions. From a plot of SHG intensity *vs.* number density relative to the reference compound, the isotropic averages $\langle\beta^2\rangle$ for **1** and **3** were extracted which are correlated to β_{zzz} by $\langle\beta^2\rangle = \frac{6}{35}\beta^2_{zzz}$ for 1D chromophores and to β_{yyy} by $\langle\beta^2\rangle = \frac{8}{21}\beta^2_{yyy}$ for D_3 symmetric molecules.[41] The accuracy of the measurements is estimated to be ±15%. The β^{B*} convention by Willets *et al*. was used throughout this paper.[42]

Cyclic voltammetry

This was performed with a conventional three electrode set-up with a Pt-disk work electrode and a Ag/AgCl pseudo-reference electrode in 0.1 M tetrabutylammonium hexafluorophosphate (TBAHFP) in MeCN under nitrogen inert gas atmosphere at room temperature. The internal standard was ferrocene (Fc/Fc^+); the scan rate was varied between 25 and 1000 mV s^{-1}. The electrochemical stability was checked by thin-layer multi-sweep experiments at 20 mV s^{-1}.

UV-Spectroelectrochemistry

This was carried out in MeCN using a thin-layer cell (100 μm) with a gold grid mini electrode described in ref. 43. This cell was coupled to a Perkin-Elmer Lambda 9 UV-Vis-NIR spectrophotometer.

Semiempirical calculations

Calculations were performed with the AM1 Hamiltonian[44] implemented in the MOPAC93[45] program package. Molecules **1–3** and the respective radical anions were optimised either at the RHF or at the UHF level as singlet, doublet, or triplet ground states, according to their spin multiplicity found in the CI calculations. The RHF wave functions were checked for UHF stability. For the radical anions of **2**, **2-OMe**, and **3**, CI calculations were performed at UHF (RHF) geometries with an active orbital space CI(*n*,*m*), where *n* = number of orbitals, *m* = number of doubly occupied orbitals. In the case of an odd number of electrons, the reference wave function was allowed to be symmetric by using the open(*n*,*m*) key word, where *n* denotes the number of electrons equally distributed over *m* orbitals. Thus, for **1**$^-$, **2**$^-$, and **2-OMe**$^-$ a CI(8,3), open(1,1), for **2**$^{2-}$ and **3**$^{2-}$ a CI(8,3), open(2,2), and for **3**$^{3-}$ a CI(8,3), open(3,3) was used. A maximum of 121 energy selected microstates is limited by the MOPAC program. The S–T and D–Q splitting energies were taken from the CI calculations without reoptimisation of the higher energy spin states because we expect the geometry differences to be minor. The absorption spectra of **1**, **2**, **2-OMe** and **3** were calculated using the VAMP6.005[46] program package at the CISD(6,3) level with all possible microstates used for the CI matrix diagonalisation. Solvent influences were taken into account at CISD(6,3) level with the SCRF method in MeCN and diethyl ether. No analysis of spin distributions was possible since the UHF wave functions of all compounds were significantly spin contaminated. The population analyses refer to Coulson charges calculated from the CI wave functions. The quadratic hyperpolarisabilities of **1** and **3** were calculated by the TDHF routine[23] implemented in MOPAC93.

Acknowledgements

We are grateful to the Fonds der Chemischen Industrie (Liebig grant to C. L.), the Deutsche Forschungsgemeinschaft (Habilitandenstipendium), the Bayerisches Staatsministerium für Unterricht, Kultus, Wissenschaft und Kunst (FORMAT Project), and the Stiftung Volkswagenwerk for financial funding, and especially to Professor J. Daub for his kind support at Regensburg.

References

1 *Chem. Rev.*, 1992, **92**, pp. 369. This issue is devoted to ET processes in biological relevant systems.
2 (*a*) S. Dapperheld, E. Steckhan, K.-H. Grosse Brinkhaus and T. Esch, *Chem. Ber.*, 1991, **124**, 2557; (*b*) F. A. Neugebauer, S. Bamberger and W. R. Groh, *Chem. Ber.*, 1975, **108**, 2406 and references cited therein; (*c*) R. Glaser, in *Acyclic Organonitrogen Stereodynamics*, eds. J. B. Lambert and Y. Takeuchi, VCH, Weinheim, 1992, p. 123.
3 (*a*) P. M. Borsenberger and D. S. Weiss, *Organic Photoreceptors for Imaging Systems*, Marcel Dekker, New York, 1993; (*b*) K. Katsuma and Y. Shirota, *Adv. Mater.*, 1998, **10**, 223; (*c*) M. Thelakkat and H.-W. Schmidt, *Adv. Mater.*, 1998, **10**, 219; (*d*) J. Pommerehne, H. Vestweber, W. Guss, R. Mahrt, H. Bässler, M. Porsch and J. Daub, *Adv. Mater.*, 1995, **7**, 551 and references cited therein.
4 (*a*) J. Fabian and H. Hartmann, *Light Absorption of Organic Colorants*, Springer, Berlin, 1980; (*b*) D. Hellwinkel, H. G. Gaa and R. Gottfried, *Z. Naturforsch.*, *Teil B*, 1986, **41**, 1045.
5 H. H. Jaffe, *J. Phys. Chem.*, 1954, **22**, 1430.
6 H. Shimamori and A. Sato, *J. Phys. Chem.*, 1994, **98**, 13481.
7 For a general introduction to nonlinear optics in organic materials, see *e.g.*: (*a*) P. N. Prasad and D. J. Williams, *Nonlinear Optical Effects in Molecules and Polymers*, Wiley, New York, 1991; (*b*) *Principles and Applications of Nonlinear Optical Materials*, eds. R. W. Munn and C. N. Ironside, Blackie Academic & Professional, Glasgow, 1993; (*c*) *Nonlinear Optics of Organic Molecules and Polymers*, eds. H. S. Nalwa and S. Miyata, CRC Press, Boca Raton, 1997; (*d*) T. J. Marks and M. A. Ratner, *Angew. Chem.*, 1995, **107**, 167; *Angew. Chem.*, *Int. Ed. Engl.*, 1995, **34**, 155; (*e*) R. G. Denning, *J. Mater. Chem.*, 1995, **5**, 365.
8 For reviews on nonlinear optics in multipolar media, see (*a*) J. Zyss and I. Ledoux, *Chem. Rev.*, 1994, **94**, 77; (*b*) J. J. Wolff and R. Wortmann, *J. Prakt. Chem.*, 1998, **340**, 99; (*c*) J. J. Wolff and R. Wortmann, *Adv. Phys. Org. Chem.*, 1999, **32**, in the press.
9 S. Stadler, F. Feiner, C. Bräuchle, S. Brandl and R. Gompper, *Chem. Phys. Lett.*, 1995, **245**, 292.
10 (*a*) R. Gleiter and W. Schäfer, *Acc. Chem. Res.*, 1990, **23**, 369; (*b*) H.-D. Martin and B. Mayer, *Angew. Chem.*, 1983, **95**, 281; *Angew. Chem.*, *Int. Ed. Engl.*, 1983, **22**, 283.
11 (*a*) E. G. McRae and M. Kasha, in *Physical Processes in Radiation Biology*, eds. L. Augenstein, R. Mason and B. Rosenberg, Academic Press, New York, 1964, pp. 23–42; (*b*) M. Kasha, H. R. Rawls and M. Asharf El-Bayoumi, *Pure Appl. Chem.*, 1965, **11**, 371; (*c*) N. Harada and K. Nakanishi, *Circular Dichroic Spectroscopy-Exciton Coupling in Organic Stereochemistry*, Oxford University

Press, Oxford, 1983, chapter X; (*d*) M. S. Gutipati, *J. Phys. Chem.*, 1994, **98**, 9750.
12 (*a*) C. Creutz, *Progr. Inorg. Chem.*, 1983, **30**, 1; (*b*) N. S. Hush, *Coord. Chem. Rev.*, 1985, **64**, 135.
13 (*a*) K. Clays and A. Persoons, *Phys. Rev. Lett.*, 1991, **66**, 2980; (*b*) K. Clays and A. Persoons, *Rev. Sci. Instrum.*, 1992, **63**, 3285.
14 K. Clays and A. Persoons, *Adv. Chem. Phys.*, 1993, **85**, 456.
15 B. C. McKusick, R. E. Heckert, T. L. Cairns, D. D. Coffman and H. F. Mower, *J. Am. Chem. Soc.*, 1958, **80**, 2806.
16 C. Reichardt, *Solvents and Solvent Effects in Organic Chemistry*, 2nd edn., VCH, Weinheim, 1990.
17 (*a*) H. B. Lueck, J. L. McHale and W. D. Edwards, *J. Am. Chem. Soc.*, 1992, **114**, 2342; (*b*) D. F. Duxbury, *Chem. Rev.*, 1993, **93**, 381.
18 (*a*) W. Verbouwe, M. Van der Auweraer, F. C. De Schryver, J. J. Piet and J. M. Warman, *J. Am. Chem. Soc.*, 1998, **120**, 1319; (*b*) G. Verbeek, S. Depaemelaere, M. Van der Auweraer, F. C. De Schryver, A. Vaes, D. Terrell and S. De Meutter, *Chem. Phys.*, 1993, **176**, 195; (*c*) L. F. Cooley, P. Bergquist and D. F. Kelley, *J. Am. Chem. Soc.*, 1990, **112**, 2612; (*d*) E. M. Kober, B. P. Sullivan and T. J. Meyer, *Inorg. Chem.*, 1984, **23**, 2098.
19 W. Liptay, R. Wortmann, H. Schaffrin, O. Burkhard, W. Reitinger and N. Detzer, *Chem. Phys.*, 1988, **120**, 429.
20 J. Bonvoisin, J.-P. Launay, M. Van der Auweraer and F. C. De Schryver, *J. Phys. Chem.*, 1994, **98**, 5052; see also correction, *ibid.*, 1996, **100**, 18006.
21 (*a*) J. L. Oudar and J. Zyss, *Phys. Rev. A*, 1982, **26**, 2016; (*b*) J. Zyss and J. L. Oudar, *Phys. Rev. A*, 1982, **26**, 2028.
22 S. Stadler, R. Dietrich, G. Bourhill, C. Bräuchle, A. Pawlik and W. Grahn, *Chem. Phys. Lett.*, 1995, **247**, 271.
23 S. P. Karna and M. Dupuis, *J. Comput. Chem.*, 1991, **12**, 487; for a review on quantum chemical calculations of NLO properties of organic and organometallic compounds, see D. R. Kanis, M. A. Ratner and T. J. Marks, *Chem. Rev.*, 1994, **94**, 195.
24 (*a*) M. Joffre, D. Yaron, R. J. Silbey and J. Zyss, *J. Chem. Phys.*, 1992, **97**, 5607; (*b*) B. M. Pierce, J. Zyss and M. Joffre, *Proc. SPIE Int. Soc. Opt. Eng.*, 1993, **2025**, 2.
25 (*a*) C. Lambert, E. Schmälzlin, K. Meerholz and C. Bräuchle, *Chem. Eur. J.*, 1998, **4**, 512; (*b*) C. Lambert, G. Nöll, E. Schmälzlin, K. Meerholz and C. Bräuchle, *Chem. Eur. J.*, 1998, **4**, 2129.
26 L.-T. Cheng, W. Tam, S. H. Stevenson, G. R. Meredith, G. Rikken and S. R. Marder, *J. Phys. Chem.*, 1991, **95**, 10631; static hyperpolarisabilities were extrapolated by the two-level approximation: J. L. Oudar and D. S. Chemla, *J. Chem. Phys.*, 1977, **66**, 2664.
27 C. M. Whitaker, E. V. Patterson, K. L. Kott and R. J. McMahon, *J. Am. Chem. Soc.*, 1996, **118**, 9966.
28 C. R. Moylan, R. J. Twieg, V. Y. Lee, S. A. Swanson, K. M. Betterton and R. D. Miller, *J. Am. Chem. Soc.*, 1993, **115**, 12599.
29 D. C. Oniciu, K. Matsuda and H. Iwamura, *J. Chem. Soc.*, *Perkin Trans. 2*, 1996, 907; see however H. Bock, A. John, Z. Havlas and J. W. Bats, *Angew. Chem.*, 1993, **105**, 416, *Angew. Chem.*, *Int. Ed. Engl.*, 1993, **32**, 416.
30 J. Cizek and J. Paldus, *J. Chem. Phys.*, 1967, **47**, 3976.
31 J. Fujita, M. Tanaka, H. Suemune, N. Koga, K. Matsuda and H. Iwamura, *J. Am. Chem. Soc.*, 1996, **118**, 9347.
32 P. M. Lahti and A. S. Ichimura, *J. Org. Chem.*, 1991, **56**, 3030.
33 For IV-CT processes in organic mixed valence systems, see (*a*) S. F. Nelsen, R. F. Ismagilov and D. R. Powell, *J. Am. Chem. Soc.*, 1996, **118**, 6313; (*b*) S. F. Nelsen, R. F. Ismagilov and D. R. Powell, *J. Am. Chem. Soc.*, 1997, **119**, 10213 and references therein: (*c*) S. F. Nelsen, R. F. Ismagilov and D. R. Powell, *J. Am. Chem. Soc.*, 1998, **120**, 1924; (*d*) J. Bonvoisin, J.-P. Launay, W. Verbouwe, M. Van der Auweraer and F. C. De Schryver, *J. Phys. Chem.*, 1996, **100**, 17079; (*e*) J. Bonvoisin, J.-P. Launay, C. Rovira and J. Veciana, *Angew. Chem.*, 1994, **106**, 2190; *Angew. Chem. Int. Ed. Engl.*, 1994, **33**, 2106; (*f*) S. F. Nelsen, *Adv. Electron Transfer Chem.*, 1993, **3**, 167.
34 Using the C–C distance for *d* involves major uncertainties because the charge is partially delocalised into the tricyanovinylphenyl rings.
35 The molar absorptivity at the highest IV-CT absorbance during reduction refers to a concentration $[M^-] = [M]_0\sqrt{K_{co}}/(2 + \sqrt{K_{co}})$ with $K_{co} = 10^{(\Delta E/0.059)}$, where ΔE is the difference of redox potentials between M^- and M^{2-}.
36 We used the method based on AM1-UHF calculations described in S. F. Nelsen, S. C. Blackstock and Y. Kim, *J. Am. Chem. Soc.*, 1987, **109**, 677.
37 C. Lambert and G. Nöll, *Angew. Chem.*, 1998, **110**, 2239; *Angew. Chem.*, *Int. Ed. Engl.*, 1998, **37**, 2107.
38 (*a*) J. E. Sutton, P. M. Sutton and H. Taube, *Inorg. Chem.*, 1979, **18**, 1017; (*b*) D. E. Richardson and H. Taube, *Coord. Chem. Rev.*, 1984, **60**, 107.
39 G. Lai, X. Bu, J. Santos and E. Mintz, *Synthesis*, 1997, 1275.
40 E. Schmälzlin, K. Meerholz, S. Stadler, C. Bräuchle, H. Patzelt and D. Oesterhelt, *Chem. Phys. Lett.*, 1997, **280**, 551.
41 (*a*) S. J. Cyvin, J. E. Rauch and J. C. Decius, *J. Chem. Phys.*, 1965, **43**, 4083; (*b*) R. Bersohn, Y.-H. Pao and H. L. Frisch, *J. Chem. Phys.*, 1966, **45**, 3184.
42 A. Willetts, J. E. Rice, D. M. Burland and D. P. Shelton, *J. Chem. Phys.*, 1992, **97**, 7590.
43 The CV solutions were transferred to a spectroelectrochemical cell described in: (*a*) J. Salbeck, I. Auerbach and J. Daub, *DECHEMA Monogr.*, 1988, **112**, 177; (*b*) J. Salbeck, *J. Electroanal. Chem.*, 1992, **340**, 169; (*c*) J. Salbeck, *Anal. Chem.*, 1993, **65**, 2169.
44 M. J. S. Dewar, E. G. Zoebisch, E. F. Healy and J. J. P. Stewart, *J. Am. Chem. Soc.*, 1985, **107**, 3902.
45 MOPAC93, Fujitsu, Japan, 1993.
46 G. Rauhut, A. Alex, J. Chandrasekhar, T. Steinke, W. Sauer, B. Beck, M. Hutter, P. Gedeck and T. Clark, VAMP6.005, Erlangen, 1996.

Paper 8/08009G